

# Structural Modifications to Polystyrene via Self-Assembling Molecules\*\*

By John C. Stendahl, Eugene R. Zubarev, Michael S. Arnold, Mark C. Hersam, Hung-Jue Sue, and Samuel I. Stupp\*

We have previously reported that small quantities of self-assembling molecules known as dendron rodcoils (DRCs) can be used as supramolecular additives to modify the properties of polystyrene (PS). These molecules spontaneously assemble into supramolecular nanoribbons that can be incorporated into bulk PS in such a way that the orientation of the polymer is significantly enhanced when mechanically drawn above the glass-transition temperature. In the current study, we more closely evaluate the structural role of the DRC nanoribbons in PS by investigating the mechanical properties and deformation microstructures of polymers modified by self-assembly. In comparison to PS homopolymer, PS containing small amounts ( $\leq 1.0$  wt.-%) of self-assembling DRC molecules exhibit greater Charpy impact strengths in double-notch four-point bending and significantly greater elongations to failure in uniaxial tension at 250 % prestrain. Although the DRC-modified polymer shows significantly smaller elongations to failure at 1000 % prestrain, both low- and high-prestrain specimens maintain tensile strengths that are comparable to those of the homopolymer. The improved toughness and ductility of DRC-modified PS appears to be related to the increased stress whitening and craze density that was observed near fracture surfaces. However, the mechanism by which the self-assembling DRC molecules toughen PS is different from that of conventional additives. These molecules assemble into supramolecular nanoribbons that enhance polymer orientation, which in turn modifies crazing patterns and improves impact strength and ductility.

## 1. Introduction

The use of glassy polymers such as polystyrene (PS) has traditionally been limited by their tendency to undergo brittle fracture.<sup>[1–3]</sup> Over the past several decades, significant efforts have been directed towards the development of additives that improve the toughness of PS and similar polymers.<sup>[4,5]</sup> Many of

these additive-based approaches to polymer toughening focus on the alteration of craze microstructure. Although crazes are usually precursors to fracture, their formation and extension under certain conditions can dissipate significant amounts of strain energy. Proper control over the nucleation and/or growth of crazes via elastomeric second-phase inclusions,<sup>[4–7]</sup> low-molecular-weight plasticization,<sup>[8–12]</sup> or alterations in chain orientation<sup>[13–15]</sup> can create “craze plasticity” in glassy polymers that significantly reduces brittleness.

We previously reported that small quantities of self-assembling molecules known as dendron rodcoils (DRCs) can be used as supramolecular additives to modify the properties of PS.<sup>[16,17]</sup> When added to monomeric styrene in amounts as low as 0.2 wt.-%, DRCs spontaneously assemble into gel-forming networks of ribbon-like structures that are  $\sim 10$  nm wide,  $\sim 2$  nm thick, and up to 10  $\mu\text{m}$  long.<sup>[18]</sup> After thermal polymerization of the styrene gels, the nanoribbons remain dispersed in small bundles throughout the polymeric solid. The presence of the nanoribbon scaffold significantly enhances the chain orientation of the polymer when it is mechanically drawn above the glass-transition temperature ( $T_g$ )<sup>[16,17]</sup> and its presence was also found to alter fracture mechanics and improve impact strengths by as much as 70 %.<sup>[16]</sup> These modifications appear to be at least partially attributable to the influence of the nanoribbons on the craze microstructures of the polymers. In the current study, we attempt to better understand the structural role of the DRC nanoribbons in PS by examining the mechanical properties and deformation microstructures of the nanoribbon-modified polymers when they are deformed in double-notch four-point bending Charpy impact (DN-4PB-CI) tests and also under uniaxial tension.

[\*] Prof. S. I. Stupp  
Departments of Materials Science and Engineering, Chemistry  
Feinberg School of Medicine, Northwestern University  
Evanston, IL 60208-3108 (USA)  
E-mail: s-stupp@northwestern.edu

J. C. Stendahl, M. S. Arnold, Prof. M. C. Hersam  
Department of Materials Science and Engineering  
Northwestern University  
Evanston, IL 60208-3108 (USA)

Prof. E. R. Zubarev<sup>[†]</sup>  
Department of Chemistry, Northwestern University  
Evanston, IL 60208-3113 (USA)

Prof. H.-J. Sue  
Department of Mechanical Engineering, Polymer Technology Center,  
Texas A&M University  
College Station, TX 77843 (USA)

[†] Current address: Department of Materials Science and Engineering,  
Iowa State University, Ames, IA 50011-2300, USA.

[\*\*] This work was supported by the U.S. Air Force Office of Scientific Research under Award No. F49620-00-1-283/P0002, the U.S. Army Research Office under Award No. DAAG55-97-1-0126, and the U.S. Department of Energy under Award No. DE-FG02-00ER45810/A001. The authors wish to recognize Yau-Ru Chen, Thang Bui, and Mark Seniw at Northwestern University for providing technical assistance and are thankful for useful discussions with Prof. Edward Kramer of the University of California at Santa Barbara.

## 2. Results and Discussion

Results from DN-4PB-CI measurements are consistent with previous data from single-notch Charpy impact tests,<sup>[16]</sup> indicating that the incorporation of small amounts of DRC nanoribbons in PS results in considerable toughening. In these measurements, PS/0.5 wt.-% DRC produced a Charpy impact strength of  $121.8 \text{ J m}^{-1}$ , compared to  $89.3 \text{ J m}^{-1}$  for PS homopolymer. An analysis of subcritically grown cracks in these specimens supports previous claims that the toughening effect of DRC nanoribbons is related to enhanced polymer-chain orientation. In PS/0.5 wt.-% DRC, the crack was short and grew in a direction perpendicular to the starter crack, but parallel to the prestrain axis and polymer-chain orientation (Fig. 1a). On the other hand, the subcritical PS homopolymer crack was substantially longer and propagated at an orientation of approximately  $10^\circ$  to the prestrain axis (Fig. 1b). These observations are consistent with DN-4PB-CI measurements and indicate there was greater resistance to crack propagation in PS/0.5 wt.-% DRC, especially normal to the direction of poly-

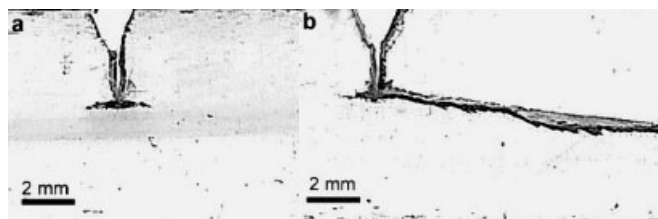


**Figure 1.** Subcritically grown cracks in DN-4PB-CI specimens: a) PS/0.5 wt.-% DRC and b) PS homopolymer.

mer-chain orientation. While the magnitude of the DRC toughening effect was slightly less in DN-4PB-CI tests than in the previous single-notch experiments<sup>[16]</sup> (36 % increase vs. 70 %, respectively), it is likely this disparity can be attributed to differences in prestraining conditions and testing geometry.

The toughening effect of DRC nanoribbons is supported by uniaxial tension experiments that highlight structural differences between DRC-scaffolded PS and the PS homopolymer. In samples prestrained to 250 % and tested in uniaxial tension at  $1.5 \text{ mm min}^{-1}$ , a significant contrast in fracture topography was observed (Fig. 2). Specimens modified by the DRC nanoribbons exhibited highly textured, yet largely homogenous, fracture surfaces that showed no clear regions of initiation or differences in propagation speed or mechanism. Although the DRC specimens are transparent in their undeformed state, these fracture surfaces were only faintly translucent due to light scattering by surface roughness and sub-surface defects. In contrast, fracture surfaces of PS homopolymer specimens exhibited classical PS fracture characteristics with central mirror-like initiation zones that transitioned to regions of planar island-like features. The island regions sometimes gave way to rougher sections on the peripheries of specimens, but these rough regions made up only small portions of the total fracture areas. Unlike DRC fractures, these regular, planar features al-

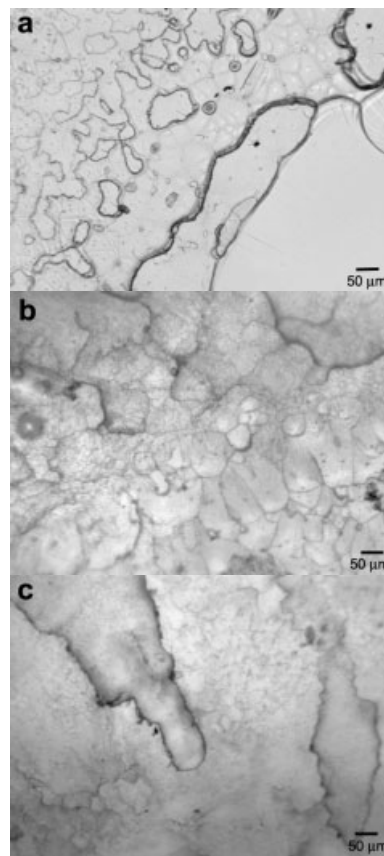


**Figure 2.** Optical micrographs of 250%-prestrained tensile fracture surfaces: a) PS homopolymer, b) PS/0.5 wt.-% DRC, and c) PS/1.0 wt.-% DRC.

lowed the homopolymers to maintain transparency after fracture. In general, the surfaces of DRC specimens had considerably greater roughness than those of PS homopolymers.

This contrast in surface topography is also revealed by atomic force microscopy (AFM) images of fracture surfaces of PS homopolymer (mirror region) and PS containing 1.0 wt.-% DRC (Fig. 3). Root-mean-square (RMS) roughness values of  $12.3 \pm 2.8 \text{ nm}$  for PS and  $102.7 \pm 23.4 \text{ nm}$  for PS/1.0 wt.-% DRC were measured from these images, indicating

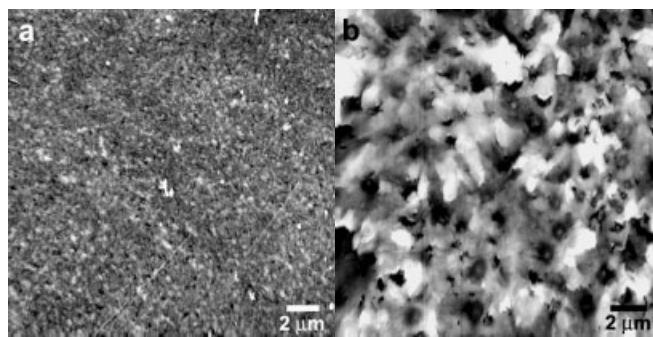


**Figure 3.** AFM images of 250%-prestrained tensile specimen fracture surfaces: a) PS homopolymer and b) PS/1.0 wt.-% DRC.

that the PS/1.0 wt.-% DRC fracture surface had almost ten times greater relief than the mirror region of the PS homopolymer surface. The increased surface area in DRC specimens suggests crack paths were highly bifurcated and likely influenced by stress concentrations at numerous cavitations and multiplanar crazes that formed ahead of crack fronts, both before crack initiation and during crack propagation.<sup>[19]</sup> In contrast, the chiefly planar features in PS homopolymer specimens indicate that most crack propagation occurred along very few large, coplanar crazes that were probably formed prior to crack initiation.<sup>[19]</sup> The mirror regions indicate that cracks initially propagated through craze layers by fibril tearing. As the cracks gained speed, they shifted to weaker material along the craze-bulk interfaces and produced the island morphologies by alternating along opposing craze wedge surfaces. These planar features in PS homopolymer suggest less plastic deformation prior to fracture than in PS/DRC specimens, and are therefore associated with higher velocity, more brittle fractures.<sup>[20]</sup>

The greater surface texture in 250 %-prestrained PS/DRC specimens was accompanied by extensive stress whitening in the sub-fracture regions, especially in 1.0 wt.-% DRC specimens (Fig. 4). Transmission optical microscopy (TOM) images of fractured cross-sections indicate that this whitening is at least partially due to the scattering of light by numerous, limited-size crazes, many of which were nucleated internally and confined to the interiors of the specimens (Fig. 5a). In contrast to the high-density crazing in DRC specimens, sub-fracture

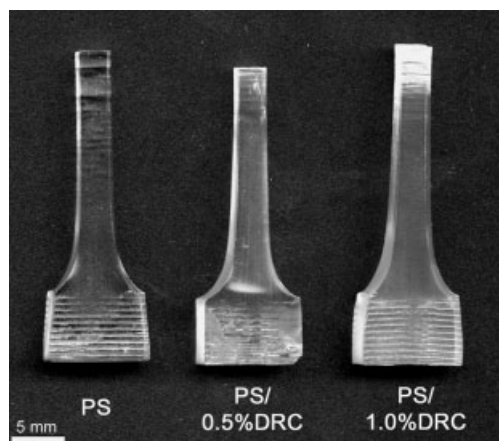


Figure 4. 250 %-prestrained tensile specimens after testing to failure at 1.5 mm min<sup>-1</sup> in uniaxial tension.

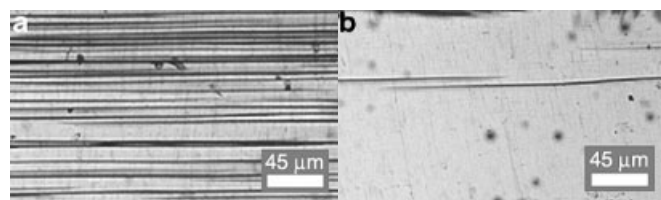


Figure 5. TOM images of craze microstructure of 250 %-prestrained specimens just below fracture surfaces: a) PS/0.5 wt.-% DRC and b) PS homopolymer.

regions in PS specimens were transparent, with significantly larger, more widely spaced crazes, some of which spanned the entire width of gauge regions (Fig. 5b). Nearly all of these crazes were associated with the exteriors of specimens and appear to have been initiated at external sites.

The smaller, higher-density crazes in DRC specimens are typical of those that form in more highly oriented polymers when stressed in tension along their axes of orientation. Although chain orientation generally tends to increase craze-initiation stresses in polymers, it eventually leads to crazes that are smaller and more numerous once the crazing threshold has been surpassed.<sup>[13-15]</sup> Ultimately, the smaller crazes in PS/DRC are desirable because they have greater stability and are less likely to initiate catastrophic failure cracks. By nucleating significantly greater numbers of crazes and producing greater total craze areas, the PS/DRC specimens should be able to dissipate larger strain energies before fracture.

Increased strain-energy dissipation via crazing is likely to be at least partially responsible for the large failure strains ( $\epsilon_f$ ) that were observed in 250 %-prestrained PS/1.0 wt.-% DRC specimens (Fig. 6). In contrast to the large increases in  $\epsilon_f$ , DRC-modified materials exhibited ultimate tensile strengths  $\sigma_{uts}$  that were only slightly, but not significantly greater than

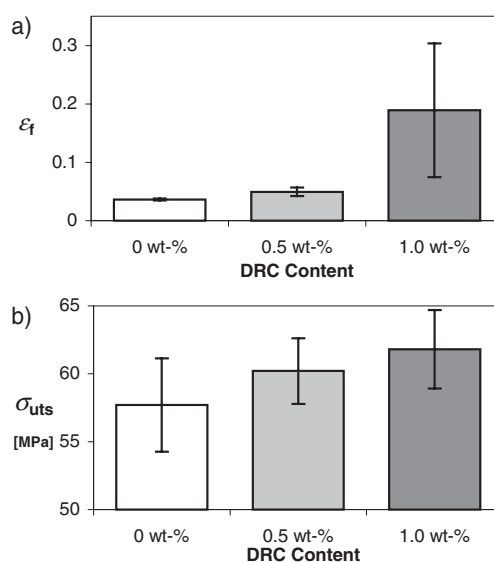
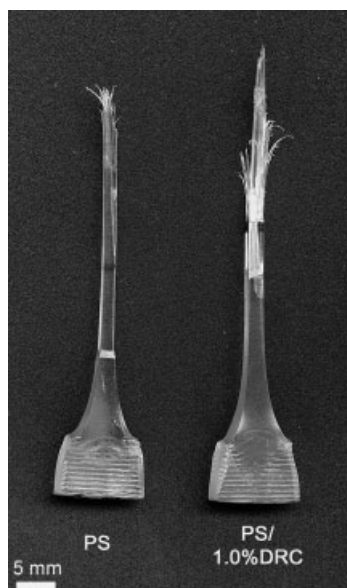


Figure 6. Average  $\epsilon_f$  and  $\sigma_{uts}$  for 250 %-prestrained PS specimens containing 0 wt.-%, 0.5 wt.-%, and 1.0 wt.-% DRC tested at 1.5 mm min<sup>-1</sup> in uniaxial tension.

those of PS homopolymer (Fig. 6). Considering DRC's influence on molecular orientation, it is fairly surprising that DRC-modified polymers were not at least moderately stronger than the less-oriented homopolymers. Multiple studies indicate that molecular orientation in polymers increases both  $\epsilon_f$  and  $\sigma_{uts}$  along the axis of orientation,<sup>[21-23]</sup> although it has also been reported that strengths are generally less sensitive to changes in orientation than failure strains.<sup>[24]</sup> Ultimately, the true significance of this result is that most other polymer modifications intended to increase ductility also reduce strengths substan-

tially.<sup>[9,25]</sup> Additives that increase ductility and maintain strength may be especially useful.

In contrast to the 250 %-prestrained fractures, completely different morphologies were observed in specimens prestrained to 1000 % and tested in uniaxial tension at 1.5 mm min<sup>-1</sup>. Instead of producing macroscopically flat fractures similar to those that occurred at 250 % prestrain, the 1000 %-prestrained specimens exhibited necking and significant fibrillation (Fig. 7). Fibers in DRC-scaffolded PS were markedly thinner and more numerous than those in PS homopolymers. The intense fibrillation in DRC-scaffolded speci-



**Figure 7.** 1000 %-prestrained tensile specimens after testing to failure at 1.5 mm min<sup>-1</sup> in uniaxial tension.

mens is consistent with expectations for a material with greater molecular orientation, since fibrous fracture is a hallmark of oriented polymers.<sup>[21,24,26]</sup> In similar fashion to the 250 %-prestrained samples, the 1000 %-prestrained PS/DRC specimens exhibited significantly more sub-surface stress whitening than PS specimens. However, this whitening appears to be largely due to voiding between fibrils, rather than crazing, which was nearly absent from all specimens. Most specimens also displayed numerous microscopic, superficial crack-like defects, but these features did not appear to be crazes due to their wide apertures and shallow depths. Although the fibrillation and lack of crazing is dramatically different than what was observed at 250 % prestrain, it is consistent with previous reports of PS drawn to strains of greater than 1000 %.<sup>[21]</sup> It is likely that the high degree of orientation in 1000 %-prestrained specimens reduced craze nucleation sites by elongating defects and also may have elevated craze-initiation stresses beyond the failure stress of the materials. At such a high degree of prestrain, the polymer chains may no longer have been able to undergo the stretching and disentanglement that is necessary to form crazes.

As a group, the 1000 %-prestrained specimens had significantly greater  $\epsilon_f$  and  $\sigma_{uts}$  than any of the 250 %-prestrained specimens (Fig. 8). This result was anticipated because higher prestrain produces greater molecular orientation and tends to

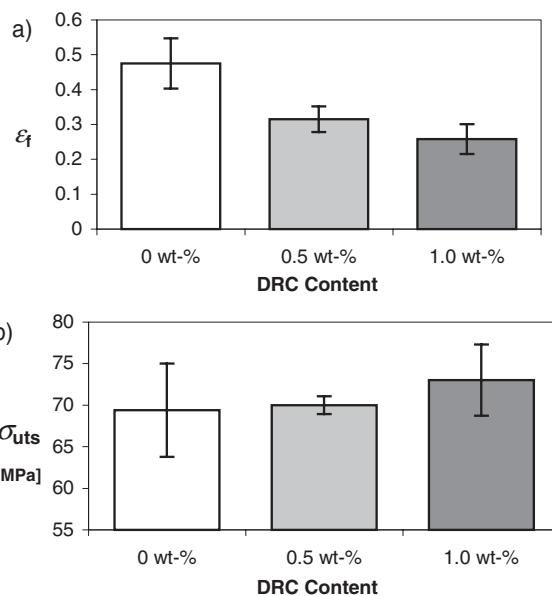


**Figure 8.** Average  $\epsilon_f$  and  $\sigma_{uts}$  for 1000 %-prestrained PS specimens containing 0 wt.-%, 0.5 wt.-%, and 1.0 wt.-% DRC tested at 1.5 mm min<sup>-1</sup> in uniaxial tension.

reduce defects.<sup>[21]</sup> However, the behavior of specimens containing DRC nanoribbons, relative to that of PS homopolymers, was substantially different in the 1000 %-prestrained group. In contrast to what was observed at 250 % prestrain, the 1000 %-prestrained specimens containing 0.5 wt.-% and 1.0 wt.-% DRC had significantly lower  $\epsilon_f$  than PS homopolymers. Although 1000 %-prestrained DRC specimens exhibited  $\sigma_{uts}$  values that were similar to those of the homopolymers, their ability to deform plastically at this high level of prestrain was significantly diminished.

In order to better understand the strain-rate sensitivity of the PS/DRC polymers, 1000 %-prestrained specimens were also tested in uniaxial tension at 20 mm min<sup>-1</sup>. The 20 mm min<sup>-1</sup> specimens exhibited even more intense fibrillation than 1000 %-prestrained specimens tested at 1.5 mm min<sup>-1</sup>, but collectively failed at slightly lower strengths and extensions (Fig. 9). Overall, however, relative results between DRC and homopolymer specimens within the two testing speed groups were similar. At 20 mm min<sup>-1</sup>, DRC specimens exhibited  $\sigma_{uts}$  that were similar to those of the PS homopolymers, but again had significantly lower  $\epsilon_f$ .

On first examination, it may seem counterintuitive that the more highly oriented DRC specimens have larger  $\epsilon_f$  than their homopolymer counterparts at 250 % prestrain, but significantly smaller  $\epsilon_f$  at 1000 %. However, it has previously been reported that there is a limit at which additional orientation in polymers actually begins to decrease  $\epsilon_f$ .<sup>[21-23]</sup> In the case of the 1000 %-prestrained DRC specimens, it is likely that this orientation limit

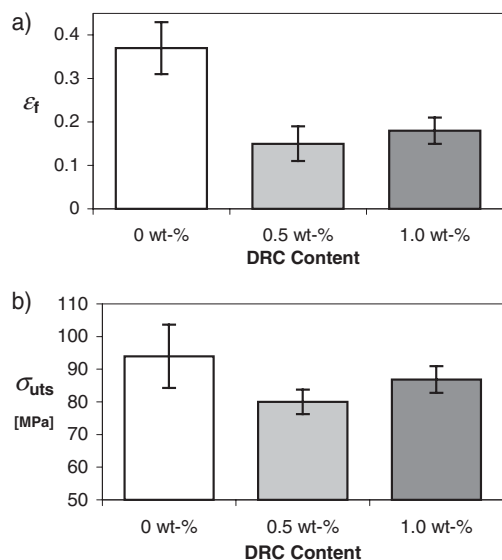


**Figure 9.** Average  $\epsilon_f$  and  $\sigma_{uts}$  for 1000%-prestrained PS specimens containing 0 wt.-%, 0.5 wt.-%, and 1.0 wt.-% DRC tested at 20 mm min<sup>-1</sup> in uniaxial tension.

has been surpassed. This decrease in  $\epsilon_f$  may be related to the disappearance of crazing at similar drawing strains, a phenomenon that occurs when craze-initiation stresses become greater than the bond-rupture stress.<sup>[21]</sup> Without the additional plasticity afforded by crazing, materials may become more brittle.

In order to better understand the orientation–property correlation in DRC-nanoribbon-scaffolded PS, specimens were also tested in their as-polymerized states without prestraining. In this case, specimens containing 1.0 wt.-% DRC actually had slightly lower  $\sigma_{uts}$  and  $\epsilon_f$  than PS homopolymers (Fig. 10). Predictably, average  $\sigma_{uts}$  values for the entire 0%-prestrained

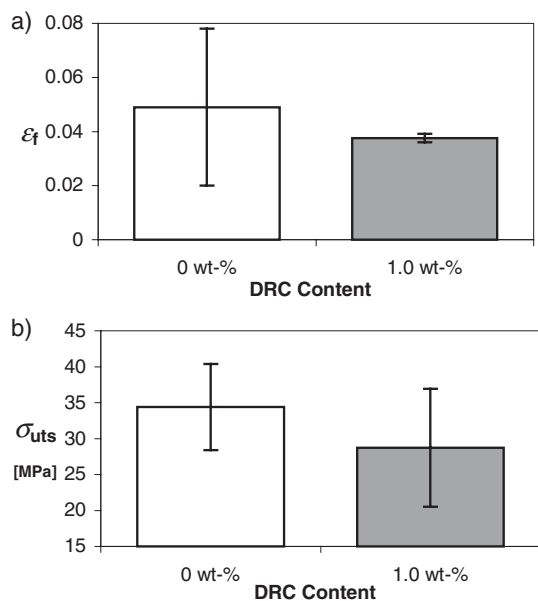


**Figure 10.** Average  $\epsilon_f$  and  $\sigma_{uts}$  for 0%-prestrained PS specimens containing 0 wt.-%, 0.5 wt.-%, and 1.0 wt.-% DRC tested at 1.5 mm min<sup>-1</sup> in uniaxial tension.

group were lower than those of the more highly oriented 250 % and 1000 % specimens. Although average  $\epsilon_f$  for the entire 0 % group were also small, they were actually similar to those for 250 %-prestrained PS and PS/0.5 wt.-% DRC. This similarity is somewhat surprising, but it is important to consider that failures in 0 %-prestrained samples occurred at considerably shorter extensions due to their smaller gauge lengths. In general, fractures in 0 %-prestrained specimens were flatter and smoother than those at larger prestrains. The 1.0 wt.-% DRC specimens exhibited more fracture surface whitening than the PS homopolymers at 0 % prestrain (Fig. 11), but did not show any of the sub-surface whitening that was observed at greater prestrains. All 0 %-prestrained specimens had extensive superficial microcracking in their

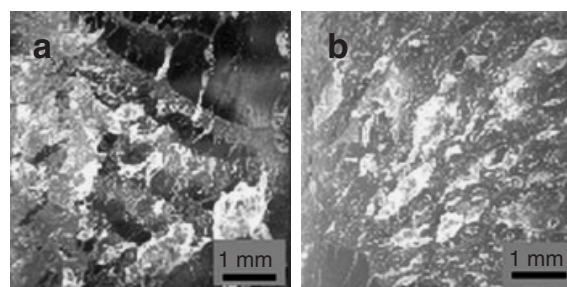


**Figure 11.** Low-magnification optical microscope images of fracture surfaces of 0%-prestrained specimens: a) PS homopolymer and b) PS/1.0 wt.-% DRC.

gauge regions, but only the PS specimens exhibited any sort of macroscopic crazing, which was only at very low levels.

Collectively, the modifications to impact strength, fracture microstructure, and ductility that were observed in PS containing self-assembling DRC molecules suggest that the supramolecular scaffold of nanoribbons has a significant structural influence on the bulk material. One important feature is the high sensitivity to degree of prestrain. DRC nanoribbons substantially increase ductility in PS at moderate prestrains, but have a negative effect without prestrain or with excessive prestrain. It is particularly interesting that oriented PS/DRC specimens exhibited both greater and lesser  $\epsilon_f$  than PS homopolymers, depending on degree of prestrain, but generally maintained  $\sigma_{uts}$  values that were comparable to the homopolymers. Another notable feature of the PS/DRC materials is that significant increases in strength were observed only in high-strain-rate Charpy impact tests and not in lower-strain-rate tensile tests. While differences in stress conditions between the two types of tests make it difficult to assert that DRC has a definite strain-rate dependence, it is clear that the incorporation of DRC provides an active strengthening mechanism in high-strain-rate Charpy impact conditions. Although these observations only provide indirect evidence of the deformation mechanisms of the DRC nanoribbons and their interactions with the bulk polymer, their relevance becomes more evident in comparisons with other types of additives used to modify PS.

Some of the most common forms of modified PS are high-impact-strength blends and copolymers in which rubbery sec-

ond phases are incorporated into the PS matrix to nucleate crazes and improve toughness.<sup>[4-7]</sup> Although this technique is also especially effective at high strain rates, it does not appear to operate by a similar mechanism to the DRC nanoribbons because it generally reduces tensile strengths by 20–40% below that of the PS homopolymer.<sup>[25]</sup> Moreover, these high-impact blends usually rely on elastomer contents that are five to thirty times greater<sup>[27]</sup> than the content of the DRC nanophases described here, and thus the materials become opaque. Although these blends show increased crazing that is similar to that observed in PS/DRC, their phase-separated microstructures are sufficiently different from the disperse DRC nanoribbon bundles<sup>[17]</sup> that it is unlikely that a common craze-initiation mechanism is shared.

Another PS-modification strategy that provides a useful comparison is the addition of low-molecular-weight diluents, such as polybutadiene, in small fractions similar to those used here with DRC.<sup>[8-12]</sup> This low-molecular-weight addition reduces craze-flow stresses and produces significant increases in ductility. Unlike DRC, however, the diluents substantially reduce tensile strengths and are not effective at high strain rates.<sup>[9]</sup> Although the DRC molecule is of the order of molecular weight that may be expected to produce a similar plasticization effect, it appears that its assembly into supramolecular nanoribbons prevents this from occurring.

### 3. Conclusions

The mechanism by which self-assembling dendron rodcoil molecules toughen PS is different from that of conventional additives. These molecules assemble into supramolecular nanoribbons that enhance polymer orientation, which in turn modifies crazing patterns and improves impact strength and ductility.

### 4. Experimental

DRC molecules were synthesized as described previously [18]. Styrene (Aldrich Chemical Company) inhibited with 10–15 ppm 4-*tert*-butylcatechol was added to glass vials containing premeasured amounts of DRC (homopolymer vials were without DRC). Sealed vials were ultrasonicated for two minutes and then warmed with a heat gun while undergoing gentle shaking. Once the DRC had dissolved, samples were heated for an additional minute to promote supramolecular self-assembly. After 10 min of ambient cooling to allow for the dissipation of excess heat, vials were transferred to a 100 °C oven for polymerization. Although vials were sealed, a nitrogen atmosphere was maintained in the oven to prevent oxidation. After 72 h, the caps were removed and vials containing the solid polymer were returned to the oven under vacuum to evaporate residual monomer. One day after removal of the caps, the vials were broken and the solid polymer cylinders were returned to the oven under vacuum. The cylinders were heated for an additional 24 h after the vials were broken and then removed from the oven and cooled to room temperature. The resulting polymers were atactic, and gel-permeation chromatography indicated the PS homopolymers and those containing DRC were of similar molecular weight.

For tensile tests, the solid PS cylinders were machined into tensile specimens with gauge dimensions 6.35 mm × 6.35 mm × 10.2 mm by a Bridgeport milling machine connected to a South Western Industries

ProtoTrack MX2 numerical controller and polished with SiO<sub>2</sub> micro-particle slurries. Prestrained specimens were drawn in uniaxial tension at 4.0 mm min<sup>-1</sup> with an MTS Sintech mechanical testing machine equipped with a heating chamber. The chamber was heated to 108 °C (slightly higher than *T<sub>g</sub>* for PS) to promote molecular orientation without chain scission or cracking. When desired lengths had been achieved, specimens were quenched with a water mist and removed from the heated chamber to preserve orientation. Undrawn specimens (0% prestrain) were tested in their as-polished states. Specimens were tested at room temperature in uniaxial tension at strain rates of 1.5 or 20 mm min<sup>-1</sup>. Error bars in all tensile strength and failure strain bar graphs represent *t* distribution confidence intervals at 90%.

For DN-4PB-CI tests, PS cylinders were machined into larger tensile specimens with gauge dimensions 20.0 mm × 8.0 mm × 27.0 mm. Tensile specimens were then prestrained at 20 mm min<sup>-1</sup> in a 112 °C chamber and quenched in water when they had reached 270% strain. The prestrained specimens were machined into bars with dimensions 3.0 mm × 8.8 mm × 110 mm. Using a 250 μm tip radius notching cutter, two 3.18 mm deep notches were cut 11.2 mm apart into the narrow face of each bar to ensure cracks propagate independently. Sharp cracks were generated at the notch tips by tapping a liquid-nitrogen-chilled razor blade. The ratio of final crack length to specimen width was held between 0.4 and 0.5. The DN-4PB-CI tests were performed on a pendulum impact tester (Model TMI-43-02) with a modified double-head striker. While a single notch is usually used in Charpy tests, previous work indicates that DN-4PB also provides an accurate measure of Charpy impact strength as long as the two cracks do not interfere [28].

AFM samples were mounted on aluminum disks with double-sided carbon tape and images (400 μm<sup>2</sup>) were collected with a ThermoMicroscopes Autoprobe CP Research AFM operating in noncontact mode. RMS roughness parameters were calculated by taking the RMS of the difference between surface height and mean surface height integrated over the sample space and divided by its area. Values were averaged for three images and presented with uncertainties of plus/minus one standard deviation.

Specimens for TOM were obtained from sub-fracture regions of 250%-prestrained tensile bars by cutting along the tensile direction. Following the procedure described by Sue et al. [29], thin sections were obtained by polishing the specimens down to approximate thicknesses of 50 μm. The thin sections were then examined using an Olympus BX60 optical microscope under bright-field setting. Images of 0%-prestrained tensile specimen fracture surfaces were obtained with a Diagnostics Instruments Spot Insight Camera connected to a Wild M3Z stereomicroscope.

Received: July 22, 2004

Final version: September 14, 2004

- [1] J. Qin, A. S. Argon, R. E. Cohen, *J. Appl. Polym. Sci.* **1983**, 28, 2319.
- [2] R. J. M. Smit, W. A. M. Brekelmans, H. E. H. Meijer, *J. Mater. Sci.* **2000**, 35, 2855.
- [3] E. J. Kramer, L. L. Berger, in *Advances in Polymer Science*, Vol. 91/92 (Ed: H.-H. Kausch), Springer, Berlin **1990**, p. 5.
- [4] C. B. Bucknall, *Toughened Plastics*, Applied Science Publication, London **1977**.
- [5] A. J. Kinloch, R. J. Young, *Fracture Behavior of Polymers*, Applied Science Publication, London **1983**.
- [6] C. B. Bucknall, R. R. Smith, *Polymer* **1965**, 6, 437.
- [7] J. A. Schmitt, H. Keskkula, *J. Appl. Polym. Sci.* **1960**, 3, 132.
- [8] O. S. Gebizlioglu, H. W. Beckham, A. S. Argon, R. E. Cohen, H. R. Brown, *Macromolecules* **1990**, 23, 3968.
- [9] J. Qin, A. S. Argon, R. E. Cohen, *J. Appl. Polym. Sci.* **1999**, 71, 1469.
- [10] A. S. Argon, *J. Appl. Polym. Sci.* **1999**, 72, 13.
- [11] A. S. Argon, R. E. Cohen, O. S. Gebizlioglu, H. R. Brown, E. J. Kramer, *Macromolecules* **1990**, 23, 3975.
- [12] H. R. Brown, A. S. Argon, R. E. Cohen, O. S. Gebizlioglu, E. J. Kramer, *Macromolecules* **1989**, 22, 1004.
- [13] N. R. Farrar, E. J. Kramer, *Polymer* **1981**, 22, 691.

- [14] C. Maestrini, E. J. Kramer, *Polymer* **1991**, 32, 609.
- [15] P. Beardmore, S. Rabinowitz, *J. Mater. Sci.* **1975**, 10, 1763.
- [16] J. C. Stendahl, L. Li, E. R. Zubarev, Y.-R. Chen, S. I. Stupp, *Adv. Mater.* **2002**, 14, 1540.
- [17] E. R. Zubarev, M. U. Pralle, E. D. Sone, S. I. Stupp, *Adv. Mater.* **2002**, 14, 198.
- [18] E. R. Zubarev, M. U. Pralle, E. D. Sone, S. I. Stupp, *J. Am. Chem. Soc.* **2001**, 123, 4105.
- [19] D. Hull, *J. Mater. Sci.* **1970**, 5, 357.
- [20] R. J. Bird, K. Mann, G. Pogany, G. Rooney, *Polymer* **1966**, 7, 307.
- [21] R. G. Cheatham, A. G. H. Dietz, *Mod. Plast.* **1951**, 29, 113.
- [22] K. J. Cleereman, H. J. Karam, J. L. Williams, *Mod. Plast.* **1953**, 30, 119.
- [23] Y. Tanabe, H. Kanetsuna, *J. Appl. Polym. Sci.* **1978**, 22, 1619.
- [24] K.-J. Choi, J. E. Spruiell, J. L. White, *Polym. Eng. Sci.* **1989**, 29, 1516.
- [25] M. Yokouchi, A. Yokota, Y. Kobayashi, *J. Appl. Polym. Sci.* **1982**, 27, 3007.
- [26] I. Wolock, S. B. Newman, in *Fracture Processes in Polymeric Solids* (Ed: B. Rosen), Interscience Publishers, New York **1964**, pp. 235–290.
- [27] D. Mathur, E. B. Nauman, *J. Appl. Polym. Sci.* **1999**, 72, 1151.
- [28] H.-J. Sue, *Polym. Eng. Sci.* **1991**, 31, 270.
- [29] H.-J. Sue, E. I. Garcia-Meitin, D. M. Pickelman, in *Elastomer Technology Handbook* (Ed: N. P. Cheremisinoff), CRC Press, Boca Raton, FL **1993**, p. 673.